Diode-end-pumped 1.2 W Yb:Y_2O_3 planar waveguide laser

Stephen J. Beecher,* Tina L. Parsonage, Jacob I. Mackenzie, Katherine A. Sloyan, James A. Grant-Jacob, and Robert W. Eason

Optoelectronics Research Centre, University of Southampton, Southampton, SO17 1BJ, UK
S.J.Beecher@soton.ac.uk

Abstract: Fabrication, characterization and laser performance of a Watt-level ytterbium-doped yttria waveguide laser is presented. The waveguide was grown onto a YAG substrate by pulsed laser deposition and features a 6 μm thick ytterbium-doped yttria layer sandwiched between two 3 μm undoped yttria layers. The laser deposited film was characterized by X-ray diffraction, showing a high degree of crystallinity and analyzed spectroscopically, showing performance indistinguishable from previously reported bulk material. When pumped with 8.5 W from a broad area diode laser the waveguide laser produces 1.2 W of output at 1030 nm.

OCIS codes: (310.0310) Thin films; (220.4610) Optical fabrication; (230.7390) Waveguides, planar; (130.0130) Integrated optics; (140.3380) Laser materials; (140.5680) Rare earth and transition metal solid-state lasers.

References and links

1. L. Xiao, X. Cheng, and J. Xu, "High-power Nd:YAG planar waveguide laser with YAG and Al_2O_3 claddings," Opt. Commun. **281**(14), 3781–3785 (2008).
2. S. P. Ng and J. I. Mackenzie, "Power and radiance scaling of a 946 nm Nd:YAG planar waveguide laser," Laser Phys. **22**(3), 494–498 (2012).
3. I. J. Thomson, F. J. F. Monjardin, H. J. Baker, and D. R. Hall, "Efficient operation of a 400 W diode side-pumped Yb:YAG planar waveguide laser," IEEE J. Quantum Electron. **47**(10), 1336–1345 (2011).
4. J. I. Mackenzie, "Dielectric solid-state planar waveguide lasers: a review," IEEE J. Sel. Top. Quantum Electron. **13**(3), 626–637 (2007).
5. E. Flores-Romero, G. V. Vázquez, H. Márquez, R. Rangel-Rojo, J. Rickards, and R. Trejo-Luna, "Planar waveguide lasers by proton implantation in Nd:YAG crystals," Opt. Express **12**(10), 2264–2269 (2004).
6. Y. E. Romanyuk, C. N. Borca, M. Pollnau, S. Rivier, V. Petrov, and U. Griebner, "Yb-doped $KY(WO_4)_2$ planar waveguide laser," Opt. Lett. **31**(1), 53–55 (2006).
7. W. Bolanos, F. Starecki, A. Benayad, G. Brasse, V. Ménard, J.-L. Doualan, A. Braud, R. Moncorgé, and P. Camy, "Tm:$LiYF_4$ planar waveguide laser at 1.9 μm," Opt. Lett. **37**(19), 4032–4034 (2012).
8. C. L. Bonner, T. Bhutta, D. P. Shepherd, and A. C. Tropper, "Double-clad structures and proximity coupling for diode-bar-pumped planar waveguide lasers," IEEE J. Quantum Electron. **36**(2), 236–242 (2000).
9. T. C. May-Smith, J. Wang, J. I. Mackenzie, D. P. Shepherd, and R. W. Eason, "Diode-pumped garnet crystal waveguide structures fabricated by pulsed laser deposition," in *Conference on Lasers & Electro-Optics/Quantum Electronics and Laser Science Conference (CLEO/QELS)* (2006), paper CMFF7.
10. K. Petermann, G. Huber, L. Fornasiero, S. Kuch, E. Mix, V. Peters, and S. A. Basun, "Rare-earth-doped sesquioxides," J. Lumin. **87–89**, 973–975 (2000).
11. R. Peters, C. Krankel, S. T. Fredrich-Thornton, K. Beil, K. Petermann, G. Huber, O. H. Heckl, C. R. E. Baer, C. J. Saraceno, T. Sudmeyer, and U. Keller, "Thermal analysis and efficient high power continuous-wave and mode-locked thin disk laser operation of Yb-doped sesquioxides," Appl. Phys. B-Lasers Opt. **102**(3), 509–514 (2011).
12. J. W. Szela, K. A. Sloyan, T. L. Parsonage, J. I. Mackenzie, and R. W. Eason, "Laser operation of a Tm:Y_2O_3 planar waveguide," Opt. Express **21**(10), 12460–12468 (2013).
13. T. C. May-Smith, A. C. Muir, M. S. B. Darby, and R. W. Eason, "Design and performance of a ZnSe tetra-prism for homogeneous substrate heating using a CO_2 laser for pulsed laser deposition experiments," Appl. Opt. **47**(11), 1767–1780 (2008).
14. K. A. Sloyan, T. C. May-Smith, and R. W. Eason, "Hybrid garnet crystal growth for thin-disc lasing applications by multi-beam pulsed laser deposition," Appl. Phys., A Mater. Sci. Process. **110**(4), 799–803 (2013).
15. Inorganic Crystal Structure Database (ICSD)," (http://icsd.cds.rsc.org).
16. F. Druon, M. Velázquez, P. Veber, S. Janicot, O. Viraphong, G. Buşe, M. A. Ahmed, T. Graf, D. Rytz, and P. Georges, "Laser demonstration with highly doped Yb:Gd_2O_3 and Yb:Y_2O_3 crystals grown by an original flux method," Opt. Lett. **38**(20), 4146–4149 (2013).

#211799 - $15.00 USD Received 19 May 2014; revised 26 Jun 2014; accepted 7 Jul 2014; published 4 Sep 2014

17. T. Taira, W. M. Tulloch, and R. L. Byer, "Modeling of quasi-three-level lasers and operation of cw Yb:YAG lasers," Appl. Opt. **36**(9), 1867–1874 (1997).

1. Introduction

Planar waveguides have proven to be an effective architecture for scaling the average power output from laser oscillators, reaching 280 W for 1064 nm Nd:YAG [1], 100 W for 946 nm Nd:YAG [2], and 400 W for 1030 nm Yb:YAG [3]. As is the case for fibers and thin disks they benefit from a high surface area to volume ratio allowing for efficient removal of heat from the laser medium [4], and also, in common with fibers and thin disks the dopant of choice for high power applications is ytterbium due to the low quantum defect. The widespread adoption of planar waveguide lasers has however been limited due, in a large part, to the difficulty of fabrication of the spatially inhomogeneous structures required for the gain media. To date, high power work has been based on crystalline waveguides due to their superior thermal properties in comparison to glass, and these have been formed, for example, by the direct bonding of precision polished crystals [2, 3]. This process is very labor-intensive, resulting in costly devices. Several other techniques exist for the fabrication of crystal planar waveguides however, and these techniques could, if the challenges can be addressed, result in high quality planar waveguide gain media at a cost that would allow this laser architecture to be more fully exploited.

Ion implantation has been shown to be capable of fabricating high quality planar waveguides [5]; however, the inability to selectively position the active laser ion in the core region precludes the fabrication of double clad structures, posing difficulties for attaining good beam quality from devices pumped by high power diode laser arrays, which typically have non-diffraction limited beam quality. Another fabrication technique, liquid phase epitaxy is capable of limiting dopant to the core regions [6, 7]; however the process is not conducive to fabrication of precise multi-layer structures with large numerical apertures (NA) suitable for high power diode laser pumps. Pulsed laser deposition combines moderately high growth rates (up to 5 μm/hour can readily be achieved), uniform planar layer deposition and the ability to accurately tailor the composition of each deposited layer. Material from a target or range of targets is ablated by a laser pulse and ejected in a plume before being deposited onto the substrate surface. It is possible to grow single crystal layers on top of crystal substrates of a very different refractive index, leading to high NA waveguides. Multi-layer guides can also be grown with double clad configurations [8], potentially leading to an output significantly brighter than the pump source used.

To date, the highest output power from a PLD grown waveguide laser is 4 W, for 50 W of pump power, reported by May-Smith at CLEO 2006 [9]. There are however, to the best of our knowledge, no other published reports of watt-level PLD waveguide lasers, and hence, in this paper we report our work towards reaching high power output from PLD grown planar waveguides. We present the growth and characterization of undoped crystalline yttria (Y_2O_3) and ytterbium-doped crystalline yttria ($Yb:Y_2O_3$) films on <100>-oriented YAG ($Y_3Al_5O_{12}$) substrates and the performance of a laser operating in this multilayer waveguide geometry. Current limitations are reported and possible solutions to these are discussed.

2. Gain media

Ytterbium doped sesquioxides $Yb:Y_2O_3$, $Yb:Sc_2O_3$ and $Yb:Lu_2O_3$ possess a desirable combination of physical and spectroscopic properties to rival or even surpass the more commonly used high power solid state laser material of choice, Yb:YAG [10]. Their widespread adoption has been hampered by the difficulty of growing high-quality crystals, which results from the high temperatures required (of order ~2400°C) to grow from the melt. Table 1 provides a comparison of some of the key attributes of Yb:YAG and $Yb:Y_2O_3$.

While the upperstate lifetimes are similar, the smaller emission cross section of $Yb:Y_2O_3$ results in the need for more than a factor of two larger population inversion to reach laser threshold. This is however partially offset by the larger absorption cross section leading to significantly lower pump saturation irradiance. For planar waveguides the absolute

#211799 - $15.00 USD Received 19 May 2014; revised 26 Jun 2014; accepted 7 Jul 2014; published 4 Sep 2014

temperature of the core is dominated by the thermal conductivity of the cladding and a high thermal conductivity for the core material should lower stress-induced losses and potentially give a small thermal lens contribution. The refractive index of Y_2O_3 is greater than YAG which allows high NA waveguides to be formed between the Y_2O_3 cores on a YAG substrate.

Table 1. Optical and mechanical properties of Yb:YAG and Yb:Y_2O_3

Material	Yb:YAG	Yb:Y_2O_3
Upper state lifetime	954 µs	850 µs
Emission cross section @1030nm	2.3 pm^2	0.9 pm^2
Absorption cross section	0.8 pm^2	2.1 pm^2
Pump saturation irradiance	28 $kW{\cdot}cm^{-2}$	11 $kW{\cdot}cm^{-2}$
Emission bandwidth (FWHM)	7 nm	12.5 nm
Quantum defect	8%	5%
Thermal conductivity for $3x10^{20}$ ions/cm^3 of Yb [11]	8.5 W/m·K	10 W/m·K
Refractive index [12]	1.82	1.91

3. Waveguide design and fabrication

In 2000 Bonner *et al.* showed that near diffraction-limited laser performance can be achieved from a highly multimode waveguide if the dopant is restricted to a region with significantly better overlap with the fundamental mode than higher order modes [8]. In this current work our waveguide was designed to have a doped core layer bounded by two nearly index-matched undoped claddings. The central layer consists of 2 at.% Yb:Y_2O_3 that is 6 µm thick, with the inner Y_2O_3 claddings either side being 3 µm-thick, giving a total waveguide thickness of 12 µm. For narrow band ($\Delta\lambda$ < 1nm), highly multimode pump light this results in an absorption length of 0.25 cm, however for a typical diode laser spectrum of 3 nm FWHM the absorption length increases to ~0.5 cm. The waveguide films were grown onto a <100>-oriented YAG substrate of dimensions 10 x 10 x 1 mm using the setup described in [12–14]. The waveguide design and backscatter scanning electron microscope image of the facet are shown in Fig. 1. The PLD layers were fabricated using a KrF excimer laser operating at a wavelength of 248 nm with pulse duration of 20 ns at a repetition rate of 20 Hz whose output was focused to achieve a fluence of 1.7 $J{\cdot}cm^{-2}$ on the Y_2O_3 and Yb:Y_2O_3 ceramic targets, which were used alternately for the respective undoped and doped layer depositions. The substrate was heated to ~900°C by a 10.6 µm CW CO_2 laser, whose Gaussian spatial output was reformatted by a ZnSe tetraprism to obtain a square beam profile [13]. During the deposition of each layer, the target was rotated, driven by an offset cam assembly, providing an epitrochoidal ablation path for efficient use of the target surface. Depositions were conducted in a background oxygen atmosphere at 4 x 10^{-2} mBar.

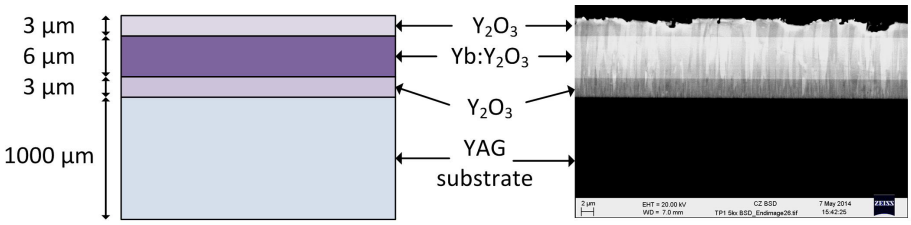

Fig. 1. The designed waveguide structure and a backscatter scanning electron microscope image of the waveguide facet. Some edge chipping from facet preparation is visible.

4. Sample characterization

4.1 Material characterization

X-ray diffraction (XRD) was performed on the multilayer waveguide structure using a Bruker D2 Phaser powder diffractometer, over a 2θ range of 10-80°. The data collected is displayed in Fig. 2(a), showing the film has grown in a highly ordered crystalline phase. The largest

#211799 - $15.00 USD Received 19 May 2014; revised 26 Jun 2014; accepted 7 Jul 2014; published 4 Sep 2014

peaks correspond to the <222> and <444> orientations of cubic yttria and the <400> and <800> peaks from the YAG substrate, the former only just visible beneath the much stronger <222> yttria peak. Other peaks, at least three orders of magnitude smaller, have been identified as being other orientations of cubic yttria, by comparison with database values [15], and peaks A and B as Kβ peaks from the XRD source corresponding to the <222> and <444> yttria peaks respectively.

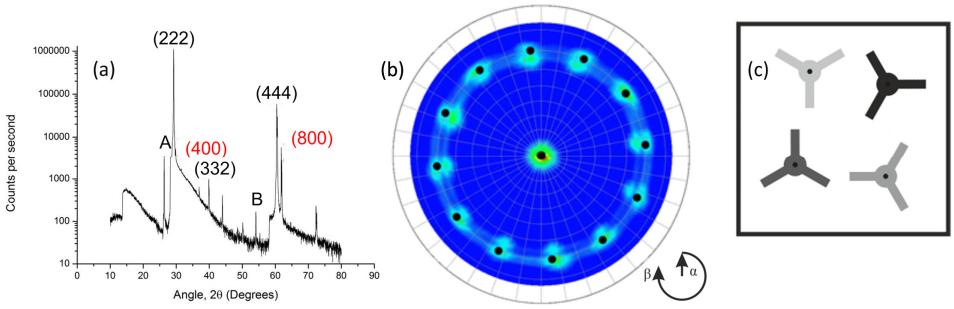

Fig. 2. (a) XRD spectrum of the 12 μm-thick Yb:Y_2O_3 multilayer waveguide. Yttria orientations are labeled in black and those from the substrate in red. (b) Pole figure of single layer Yb:Y_2O_3 grown on <100> YAG with overlay (black dots) of predicted (222) pole figure with <111> orientation. (c) Illustration of possible island domain growth.

Figure 2(b) presents a (222) pole figure of a single layer of Yb:Y_2O_3 grown on <100>-oriented YAG, showing 12 peaks separated equally by 30° in β with an α value of 18°. The peaks indicate that the crystalline film has four distinct rotationally-orientated domains about the <111> direction, since a simulated (222) pole figure for a single domain with cubic symmetry shows three fold symmetry, and hence three separate peaks. The diffuse scattering observed around each of the measured peaks indicates a small number of other orientations around <111> and the splitting indicates a tilt away from ideal <111>-orientation. This indication of the presence of four different domain orientations will likely lead to structural inhomogeneity within the crystal, particularly at the domain boundaries, contributing to increased propagation loss above what would be expected from a single-domain sample.

Energy dispersive x-ray analysis (EDX) was used to characterize the dopant concentration and profile through the multilayer waveguide by taking measurements across a facet. Ytterbium was only detected in the waveguide core, with a concentration of 1.85 at.%. Following material characterization, two opposing facets of the waveguide structure were polished plane-parallel for laser experiments, resulting in a final waveguide length of ~8 mm.

4.2 Spectroscopic characterization

Light from a 965 nm diode laser was loosely focused to a 0.5 mm radius spot on the face of a 12 μm single Yb:Y_2O_3 layer, grown under the similar conditions to the multilayer guide, on a YAG substrate. The diode laser was pulsed at a repetition rate of 10 Hz with a peak power of 1 W, resulting in a peak irradiance of ~125 W·cm^{-2}, significantly below the saturation intensity for the material. Fluorescence from the Yb:Y_2O_3 film was collected and then refocused onto a photodiode with a 1 μm long pass filter used to remove pump light. The decay of the fluorescence was exponential with a lifetime of 860 μs, see Fig. 3(a), consistent with the measured lifetime of this material grown by other methods [10]. For measurement of the fluorescence spectrum, the 965 nm diode laser was focused to a spot, with second moment beam widths of 10 μm x 800 μm, at one facet of the waveguide. Fluorescence emerging from the top face of the sample, adjacent to the facet through which the incident pump light was coupled, was captured by a proximity-coupled 62.5 μm core diameter 0.22 NA multimode fiber connected to an optical spectrum analyzer (ANDO AQ6317B). This collection configuration minimizes the distance that the fluorescence must travel through doped material, reducing spectral-dependent reabsorption. The Füchtbauer-Ladenburg equation was

#211799 - $15.00 USD Received 19 May 2014; revised 26 Jun 2014; accepted 7 Jul 2014; published 4 Sep 2014

used to calculate the emission cross section, and McCumber analysis was then used to calculate the absorption cross section for the material using Stark levels calculated from data in [16], see Fig. 3(b). It should be noted that some pump light scattered from the guide was visible in the fluorescence spectrum, so this 3 nm spectral region on the blue side of the zero phonon line was removed from the fluorescence data and then linearly interpolated before analysis.

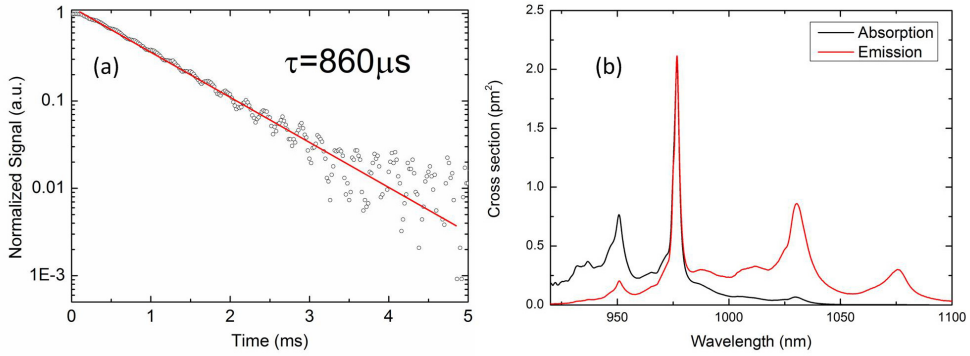

Fig. 3. Spectroscopic characterization of a Yb:Y_2O_3 PLD grown film: (a) fluorescence lifetime, and (b) absorption and emission cross sections.

5. Laser experiments

The waveguide was mounted on a 5-axis translation stage (3 spatial dimensions, roll and yaw). A pump input mirror (HT 950-990, HR 1020-1100) was placed close to one facet and an output coupler close to the opposite waveguide facet, creating a quasi-monolithic plane-plane cavity. Light from the broad area diode laser was coupled into the waveguide with the fast axis focused to a radius of 5 μm to couple into the guided dimension and the slow axis quasi-collimated at a radius of 400 μm, as shown in Fig. 4(a). The pump power was controlled using a half waveplate and polarizing beam splitter and the laser output was reflected from an HT 950-990, HR 1020-1100 mirror to remove any unabsorbed pump light before being measured by a thermal power meter, the pump reflectivity at the angle of incidence used was measured to be significantly below 1%. Three output couplers were trialed with reflectivities of 95%, 75% and 30%, see Fig. 4(b): in all cases the laser wavelength was 1030 nm with laser thresholds of 2.0, 2.25 and 2.5 W respectively. A laser threshold analysis, based on the formulism reported by Taira *et al.* [17], results in a parasitic cavity loss of 2.2 dB per round trip. By assuming this to be entirely due to waveguide propagation loss, an estimate of 1.4 dB·cm^{-1} is obtained. The output power was highest for the 30% reflectivity output coupler and with the polarizing beam splitter removed, to obtain a final power measurement at the full available incident pump power of 8.5 W (after lenses and pump input mirror), yielded a maximum waveguide laser output of 1.2 W, see Fig. 5.

After output power characterization, the laser output was imaged on to a CMOS detector array. The intensity distribution in the guided dimension followed a Gaussian profile displaying a nearly diffraction limited beam quality, M^2 = 1.2. The non-guided axis showed significant intensity variation across the beam. The same spatial variation was observed when a HeNe laser beam was coupled into the guide and the transmitted beam reimaged onto the same CMOS camera. It is evident that the PLD-grown Y_2O_3 shows a strong preference for <111>-oriented growth, see Fig. 2(a) and [12], and use of a <100>-oriented YAG substrate allows for four potential crystal growth directions. We believe that islands of differently orientated epitaxially grown yttria are merging during the growth process and defects, porosity and strain occur at the grain boundaries leading to the significant value of propagation loss, and the resultant observed poor beam quality in the non-guided axis.

#211799 - $15.00 USD Received 19 May 2014; revised 26 Jun 2014; accepted 7 Jul 2014; published 4 Sep 2014

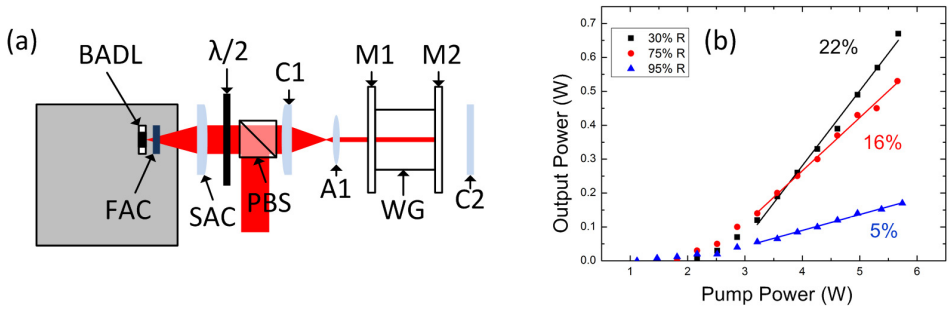

Fig. 4. (a) Schematic of the optical layout: BADL, broad-area diode laser; FAC, fast axis collimator; SAC, slow axis collimator; λ/2, half waveplate; PBS, polarizing beam splitter; C1 & C2, cylindrical lenses; A1, aspheric lens; M1, pump input mirror; WG, waveguide; M2, output coupler. (b) Laser performance as a function of pump power for three different output couplers.

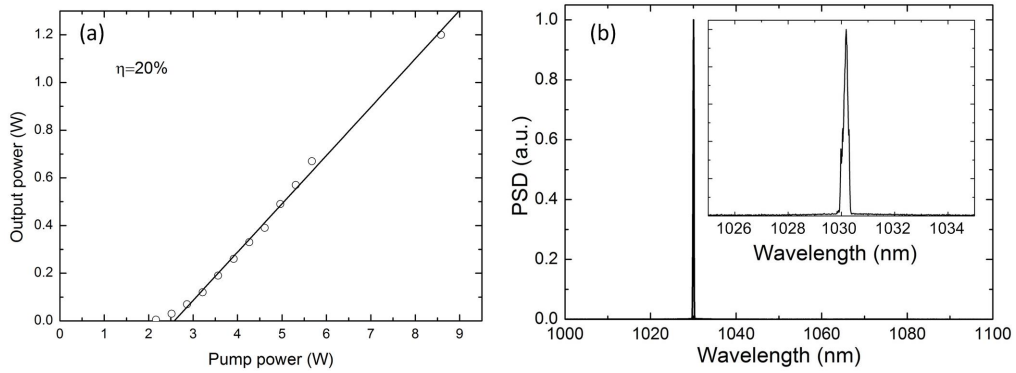

Fig. 5. (a) Laser performance for the 30% reflectivity output coupler. (b) Typical laser spectrum, inset shows spectrum over the range of 1025 nm to 1035 nm.

6. Conclusions

We have demonstrated watt-level output from a PLD-grown crystalline Yb:Y_2O_3 on YAG waveguide with no negative thermal effects observed up to the incident pump power of 8.5 W. We believe the majority of the waveguide propagation loss is caused by the Y_2O_3 growing in four possible orientations in the plane of the guide, with scattering occurring from porosity and defects at the grain boundaries. By appropriate selection of a waveguide substrate this loss should be significantly reduced. To date however, yttria growth on <111>-orientated YAG has resulted in waveguides with higher loss, likely due to the intrinsic lattice mismatch between these materials and the orientational misalignment that can ensue. Further optimization of the fabrication process should lead to lower propagation losses and significant reduction in scattering from grain boundaries, allowing for the construction of efficient lasers and amplifiers.

Acknowledgments

The authors acknowledge the support of the EPSRC through grant nos. EP/L021390/1, EP/H005412/1 and EP/J008052/1. Thanks to Dr Mark Light, School of Chemistry, University of Southampton, for assistance in pole figure measurements and interpretation.

#211799 - $15.00 USD Received 19 May 2014; revised 26 Jun 2014; accepted 7 Jul 2014; published 4 Sep 2014